Genome downsizing, physiological novelty, and the global dominance of flowering plants

Kevin A. Simonin[1*] and Adam B. Roddy[2]

[1]San Francisco State University, Department of Biology, San Francisco, CA, 94132, USA

[2]Yale University, School of Forestry and Environmental Studies, New Haven, CT, 06511, USA

*Correspondence to: simonin@sfsu.edu

Summary

During the Cretaceous (145-66 Ma), early angiosperms rapidly diversified, eventually outcompeting the ferns and gymnosperms previously dominating most ecosystems. Heightened competitive abilities of angiosperms are often attributed to higher rates of transpiration facilitating faster growth. This hypothesis does not explain how angiosperms were able to develop leaves with smaller, but densely packed stomata and highly branched venation networks needed to support increased gas exchange rates. Although genome duplication and reorganization have likely facilitated angiosperm diversification, here we show that genome downsizing facilitated reductions in cell size necessary to construct leaves with a high density stomata and veins. Rapid genome downsizing during the early Cretaceous allowed angiosperms to push the frontiers of anatomical trait space. In contrast, during the same time period ferns and gymnosperms exhibited no such changes in genome size, stomatal size, or vein density. Further reinforcing the effect of genome downsizing on increased gas exchange rates, we found that species employing water-loss limiting crassulacean acid metabolism (CAM) photosynthesis, have significantly larger genomes than C3 and C4 species. By directly affecting cell size and gas exchange capacity, genome downsizing brought actual primary productivity closer to its maximum potential. These results suggest species with small genomes, exhibiting a larger range of final cell size, can more finely tune their leaf physiology to environmental conditions and inhabit a broader range of habitats.

Introduction

The abrupt origin and rapid diversification of the flowering plants during the mid-Cretaceous, and their eventual dominance globally, has long been considered an 'abominable mystery' [1]. While the cause of their high diversity has been attributed primarily to coevolution with pollinators and herbivores, many hypotheses have been posed to explain why angiosperms were able to become ecologically dominant in most terrestrial ecosystems. A common theme among these hypotheses has been the idea that angiosperms developed a set of physiological traits that allowed them to achieve higher rates of primary productivity than either the ferns or the gymnosperms [2]. Terrestrial primary productivity is determined by the photosynthetic capacity of leaves, and one of the greatest biophysical limitations to photosynthetic rates across all the major clades of terrestrial plants is the leaf surface conductance to CO_2 and water vapor. In order for CO_2 to diffuse from the atmosphere into the leaf, the wet internal surfaces of leaves must be exposed to the dry ambient atmosphere, which can cause leaf desiccation and prevent further CO_2 uptake. As a consequence, increasing leaf surface conductance to CO_2 also requires increasing rates of leaf water transport in order to avoid desiccation[3].

Both theory and empirical data suggest that among all major clades of terrestrial plants the upper limit of leaf surface conductance to CO_2 and water vapor is tightly coupled to biophysical limitations on cell size [4-7]. Cellular allometry, in particular the scaling of genome size, nuclear volume, and cell size represents a direct physical constraint on the number of cells that can occupy a

given space and, as a result, on the distance between cell types and tissues [8]. Because leaves with many small stomata and a high density of veins promote higher rates of gas exchange than leaves with fewer, larger stomata and larger, less dense veins [9], variation in cell size can drive large changes in potential carbon gain [10]. Without reducing cell size, increasing stomatal and vein densities would displace other important tissues, such as photosynthetic mesophyll cells [11]. Therefore, the densities of stomata on the leaf surface and of veins inside the leaf are inversely related to the sizes of guard cells and xylem elements of which they are comprised.

While numerous environmental and physiological factors can influence the final sizes of somatic eukaryotic cells, the minimum size of meristematic cells and the rate of their production are strongly constrained by nuclear volume, more commonly measured as genome size [12-15]. Among land plants, the bulk DNA content of cells varies by three orders of magnitude, with the angiosperms exhibiting both the largest range in genome size and the smallest absolute genome sizes [16]. Whole-genome duplications and subsequent genomic rearrangements rapidly change genome size and are thought to have directly contributed to the unparalleled diversity in anatomical, morphological, and physiological traits of the angiosperms [15,17-21]. We extend this prior work and predict that genome size variation is not only responsible for gene diversification but also directly controls minimum cell size and, thus, is the underlying variable directly influencing both stomatal size and density and leaf vein density thus directly influencing rates of leaf gas exchange across the major clades of terrestrial plants.

To test whether genome downsizing among the angiosperms drove the anatomical and physiological innovations that resulted in their ecological dominance over other major clades of terrestrial plants, we compiled data for genome size, cell size (guard cell length, l_g), leaf vein density (D_v), and maximum and operational leaf surface conductance to CO_2 and water vapor ($g_{s,max}$ and $g_{s,op}$, respectively) for almost 1100 species of ferns, gymnosperms, and angiosperms. If genome downsizing were critical for angiosperm success, then we expect genome size to have declined rapidly during early angiosperm evolution but, perhaps, to have remained unchanged among the ferns and gymnosperms. Furthermore, if genome size constrains l_g and D_v, then evolutionary changes in genome size should precede changes in both l_g and D_v. Finally, we predict that the benefits of genome downsizing on carbon gain should be greatest when photosynthesis and transpiration are proportional, such as in plant species that possess C3 and C4 photosynthetic metabolism, in contrast to species employing crassulacean acid metabolism (CAM), which decouples gas exchange from periods of high evaporative demand. If these predictions about the biophysical effects of genome size and its evolution are supported, then genome downsizing among the angiosperms led directly to their greater potential and realized primary productivity, contributing to their rapid domination of ecosystems globally.

Results

Trait correlations (genome vs vein density and cell size) and phylogenetic independent contrasts

Genome size varied substantially among major clades (Figure 1) and was a strong predictor of anatomical traits across the major groups of terrestrial plants even when accounting for phylogeny. Genome size explained 42% of between species variation in l_g across the major groups of terrestrial plants (Figure 2a). Additionally, a single relationship predicted l_g from genome size across all species. Similarly, a strong negative correlation existed between genome size and both D_s (Figure 2b; $R^2 = 0.32$) and D_v (Figure 2c; $R^2 = 0.46$). Among major clades and within the angiosperms, traits showed strong, significant correlations between PICs, highlighting the coordinated evolution of these traits repeatedly throughout the history of seed plants (Table S2).

Biophysical scaling relationships: maximum and operational leaf surface conductance

Within clades, only the angiosperms exhibited a significant relationship between genome size and either $g_{s,\,max}$ or $g_{s,\,op}$. Sample sizes among the ferns and gymnosperms for these traits were quite low, precluding statistical significance. Yet, ferns and gymnosperms fell within the ranges of $g_{s,\,max}$ and $g_{s,\,op}$ defined by the angiosperms. The global scaling relationships among all species between genome size and either $g_{s,max}$ or $g_{s,op}$ were not significantly different than those for only the angiosperms, suggesting that a single relationship may exist between genome size and stomatal conductance (Figure 3).

Regardless of the leaf thickness (70, 100, 130 μm) used to calculate $g_{s,op}$, the scaling relationships between genome size and $g_{s,op}$ were significantly steeper than the relationship between genome size and $g_{s,max}$ (all $P < 0.001$). Therefore, across species, shrinking the genome brings $g_{s,op}$ closer to $g_{s,max}$ (Figure 3, Table 1).

126

127 *Trait evolution through time*

128 Compared to the ferns and gymnosperms, genome sizes, D_v, and l_g of the
129 angiosperms all evolved into new regions of trait space during the Cretaceous (Figure 4),
130 increasing rates of carbon assimilation and ushering in more rapidly growing forests. For
131 all three traits, the logarithmic curve fit the extreme values better than a linear
132 relationship (genome size **Δ**AIC = 12.89; D_v **Δ**AIC = 11.43; l_g **Δ**AIC = 24.69). In contrast
133 to the angiosperms, fern and gymnosperm lineages exhibited no such change in any of
134 the traits during the Cretaceous. For fern and gymnosperm traits, the linear fit including a
135 slope and intercept was not significantly better than the model lacking a slope (i.e. the
136 mean reconstructed trait value), except for fern minimum l_g, which was better modeled by
137 a linear regression with a slope, although this model indicated that fern l_g increased
138 through time (Figure 4).

139 Genome size evolution among C3 species was best modeled by allowing for
140 different rates of trait evolution for the three clades, consistent with our prediction that
141 the angiosperms capitalized on genome downsizing. Although we had predicted that OU
142 models, which model stabilizing selection around optimum trait values, would best fit the
143 data, the best-fitting model was instead the Brownian motion model that included
144 different rates for each clade. In this model, the rate parameter indicates the standard
145 deviation of trait values around the phylogenetic mean; thus a faster rate is indicative of
146 greater trait variance. In all 100 simulations, the Brownian motion model provided the
147 best fit with **Δ**AIC = 14.33 ± 0.17, compared to the second-best fitting model in each
148 iteration (Table 2). Across all C3 taxa, genome size evolved faster in the ferns (0.19 ±

149 0.0009) and gymnosperms (0.14 ± 0.0008) than in the angiosperms (0.088 ± 0.0006).
150 Similarly, in the combined analysis that incorporated all clades and photosynthetic
151 pathways, a Brownian motion model with multiple rates best described the data in all 100
152 simulations (**Δ**AIC = 130.14 ± 1.20), and the modeled parameters were similar to those
153 from the other models (Table 2).

154 Among the angiosperms, genome size evolution differed with photosynthetic
155 pathway, reflecting that genome size-cell size allometry imposes different constraints on
156 C3 and CAM species (Figures 1, 5). First, genome size evolution was best modeled by a
157 Brownian motion process (100 out of 100 simulations, **Δ**AIC = 102.39 ±1.04; Table 2)
158 that allowed for multiple rates of evolution for lineages employing the different
159 photosynthetic pathways. CAM lineages had the largest estimated phylogenetic mean
160 genome size (equivalent to the estimated ancestral genome size) and also the fastest rate
161 of genome size evolution, in both balanced (phylogenetic mean: $t = 18.61$, df = 105.11, P
162 < 0.0001; rate: $t = 35.36$, df = 99.65, P < 0.0001) and unbalanced (phylogenetic mean: $t =$
163 30.89, df = 113.66, P < 0.0001; rate: $t = 47.53$, df = 100.99, P < 0.0001) species sampling
164 (Figure 4). Second, we tested whether there were time lags between shifts in genome size
165 and shifts in either D_v or l_g associated with transitions between photosynthetic pathways.
166 If genome size fundamentally constrains D_v and l_g, then shifts in genome size should
167 either coincide with or precede shifts in the other traits, but genome size should not lag
168 behind either D_v or l_g. Although in 96 of 100 simulations vein density lagged behind
169 genome size, support for this model was weak (ΔAIC = 2.80 ± 0.16), suggesting that
170 there has been little or no lag between D_v and genome size. Similarly, although shifts in l_g
171 lagged behind shifts in genome size in 80 of 100 simulations, support was weak (ΔAIC =

172 0.99 ± 0.09). In the other 20 simulations, there was no lag between shifts in genome size
173 and l_g (ΔAIC = 1.32 ± 0.45), further suggesting that genome size and cell size evolve in
174 unison. In none of the time lag simulations did genome size lag behind either D_v or l_g,
175 strengthening support for genome size fundamentally constraining both l_g and D_v.
176
177 **Discussion**
178 Our results suggest that the basis for developing leaves with the potential
179 for high rates of gas exchange derive not exclusively from common
180 developmental programs nor from genetic correlations (i.e. linkage between genes
181 controlling both traits), but, even more fundamentally, from biophysical scaling
182 constraints that limit minimum cell size [4,38]. These scaling relationships between
183 genome size and gas exchange rates as well as analyses of trait evolution suggest
184 that genome downsizing among the angiosperms permitted the evolution of the
185 anatomical traits responsible for increased rates of photosynthesis and biomass
186 accumulation (Figures 2-4). Importantly, while genome downsizing has been
187 critical to increasing leaf gas exchange rates among the angiosperms, it was not a
188 key innovation that occurred only at the root of the angiosperm phylogeny.
189 Rather, the angiosperms exhibit a wide range of genome sizes, and coordinated
190 changes in genome size and physiological traits have repeatedly occurred
191 throughout the evolutionary history of the angiosperms (Table S2). Whole-
192 genome duplications have been particularly important in promoting
193 diversification among the angiosperms [17] yet result in larger, physiologically

194 detrimental, genomes. Our results suggest that genome downsizing is critical to
195 recovering leaf gas exchange capacity subsequent to genome duplications.
196 The ecological revolution ushered in by the angiosperms is due largely to
197 the biophysical benefits associated with decreasing genome and cell sizes. If
198 heightened competitive ability among the angiosperms drove their ecological
199 dominance, then innovations that allowed minimum cell size to decline were
200 critical to this transformative process [38]. Because genome size provides a
201 boundary on minimum cell size, genome size has numerous consequences for the
202 structure and organization of cells and tissues in leaves, which directly influence
203 metabolic rates. Specifically, unlike ferns and gymnosperms, angiosperms were
204 able to develop leaves with numerous, small stomata and a high density of veins
205 because of rapid reductions in genome size during the Cretaceous (Figures 2, 4).
206 Non-angiosperm lineages exhibited no similar changes in these traits during the
207 same time, despite a single, universal scaling relationship in all major clades of
208 terrestrial plants between genome size and anatomical (D_v and l_g) and
209 physiological ($g_{s,max}$ and $g_{s,op}$) traits. Across seed plants, genome downsizing
210 effectively brings actual productivity closer to its theoretical maximum (Figure 3),
211 allowing the angiosperms to outcompete other land plants.
212 Cell size has direct and predictable effects on gas diffusion across the leaf
213 epidermis, and, as we show here, also on the supply of liquid water to the leaf.
214 Physical resistance to diffusion across leaf surfaces is ultimately determined by
215 the size of epidermal cells, and the maximum diffusive conductance of CO_2 and
216 water vapor ($g_{s,max}$) is higher in leaves with numerous, small stomata [4,6,7]. While

217 the effects of cell size on leaf epidermal properties have been well characterized,
218 the effects of cell size on the efficiency of liquid water supply through the leaf
219 are, perhaps, less obvious. Given a constant leaf volume, increasing D_v without
220 displacing photosynthetic mesophyll cells requires reductions in vein and conduit
221 sizes that can only be accomplished by decreasing cell size [11,39]. However, smaller
222 conduits have higher hydraulic resistances. To overcome the increase in resistance
223 associated with reducing conduit sizes, other innovations in xylem anatomy that
224 reduce hydraulic resistance have been hypothesized to facilitate narrower xylem
225 conduits and high D_v. In particular, the development of low resistance end walls
226 between adjacent cells is thought to have given angiosperms a hydraulic
227 advantage as conduit diameters decreased. Only in angiosperm lineages with very
228 high D_v do primary xylem have simple perforation plates, which have lower
229 resistance to water flow than scalariform perforation plates [11]. Similarly, the low
230 resistance of gymnosperm torus-margo pits compared to angiosperm pits can
231 result in higher xylem specific hydraulic conductivity for small diameter conduits
232 [40]. In both cases, while smaller conduits have higher resistance, this potential cost
233 has been offset by other innovations that reduce hydraulic resistance at the scale
234 of the whole xylem network. The requirement of these other changes to xylem
235 anatomy to occur before potential gains from reduced conduit sizes can be
236 realized may explain why evolutionary shifts in D_v almost always lagged behind
237 shifts in genome size associated with transitions between photosynthetic
238 pathways. In contrast, shifts in l_g were less likely to lag behind shifts in genome

size, instead evolving concurrently with genome size, probably due to the direct and simple effect of genome size on l_g without the need for other traits to evolve.

While genome size limits minimum cell size, final cell size can vary greatly as cells grow and differentiate. After cell division and during cell expansion, various factors influence how large a cell becomes. Intracellular turgor pressure overcomes the mechanical rigidity of the cell wall to enlarge cellular boundaries. The magnitude of turgor pressure is itself controlled by water availability around the cell and the osmotic potential inside the cell. Final cell size is controlled therefore by both biotic and abiotic factors that influence pressure gradients in and around the cell. By reducing the lower limit of cell size, genome downsizing expands the range of final cell size that is possible. Thus, species that can vary cell size across a wider range can more finely tune their leaf anatomy to match environmental constraints on leaf gas exchange. Indeed, D_v, l_g, and stomatal conductance are more variable among species with small genomes, and the variance in these traits unexplained by genome size is likely due to environmental variation (Figures 2-4), although analyses of intraspecific genome size variation are needed to further clarify the potential links between genome size variation and environmental variation. Interestingly, only the angiosperms occupy this region of trait space, and the angiosperms tend to be more productive than either the ferns or the gymnosperms across a broad range of environmental conditions. Furthermore, genome size may predict ecological breadth even within species insofar as species with small genomes can exhibit greater plasticity in final cell size and inhabit a wider range of environmental conditions. Thus, rapid

genome downsizing by the angiosperms during the Cretaceous likely explains not only their greater potential and realized primary productivity (Figure 3) but also why they were able to expand into and create new ecological habitats, fundamentally altering the global biosphere and atmosphere [41].

Yet, not all angiosperms have small genomes (Figures 1-2). Genome size-cell size allometry determines physiological function within a given environment when photosynthetic rates are proportional to transpiration rates. This is certainly the case for species employing the C3 and C4 photosynthetic pathways. However, due to higher water use efficiency of C4 photosynthesis, the physiological effects of genome size variation may be slightly weaker in C4 species than they are in C3 species, as reflected in the slightly larger genomes and guard cell lengths of C4 species. Nonetheless, D_v and photosynthetic metabolism in many C4 plants are intimately linked due to the physical arrangement of the sites of carboxylation into a layer of cells surrounding the veins (i.e. bundle sheath cells). Because of this physical association, increasing the number of cells that are able to assimilate CO_2 requires an increase in the number of veins. In contrast to both C3 and C4 photosynthetic metabolism, species employing CAM photosynthesis effectively decouple carbon uptake from periods of relatively high evaporative demand. For CAM species, the constraints of genome size on the coordination between carbon gain and water loss are minimal, and, as a result, CAM species have significantly larger genomes than either C3 or C4 species (Figures 4-5). CAM lineages also have faster rates of genome size evolution than C3 lineages, suggesting that genome size may be more constrained in C3 lineages because cell size has a direct

285 and substantial effect on gas exchange rates (Figure 5). However, the limited
286 taxonomic resolution of CAM photosynthesis may be biasing our estimates of
287 evolutionary rates. There are undoubtedly C3 species and C3-CAM intermediates
288 that we have classified as strictly CAM, which would increase the disparity in
289 genome size and lead to an underestimation of the difference in genome size
290 between C3 and CAM species but an overestimation of the rate of genome size
291 evolution among species classified as strictly CAM. Nonetheless, the difference in
292 genome size between extant C3 and CAM species highlights the fundamental
293 importance of genome downsizing in raising the limits of leaf gas exchange when
294 carbon uptake is directly coupled to water loss. By no means should this trivialize
295 the ecological importance of CAM photosynthesis. Rather, it reinforces the
296 innovativeness of the angiosperms because genome downsizing is not the only
297 strategy conferring ecological success; CAM photosynthesis, regardless of
298 genome size, has allowed colonization of marginal environments often
299 uninhabitable by C3 species.
300

301 **Conclusion**

302 The rapid diversification and spread of angiosperms during the Cretaceous
303 dramatically restructured terrestrial ecosystems [41,42]. While their heightened
304 diversification rates have long been thought to result from a combination of
305 unique traits that allowed them to coevolve with pollinators and herbivores [43-47],
306 only recently have hypotheses about how angiosperms became ecologically
307 dominant been considered. Central to these hypotheses has been that the

308 angiosperms became competitively more successful due to faster growth rates [48],
309 supported by higher rates of photosynthesis and transpiration [9,30,42]. Anatomical
310 innovations that appeared among the angiosperms–smaller, more abundant
311 stomata and narrower, more densely packed leaf veins–that support higher rates of
312 transpiration and photosynthesis would have been particularly advantageous as
313 atmospheric CO_2 concentration declined during the Cretaceous. These traits are
314 unique to the angiosperms and due, we show, to reductions in cell and genome
315 sizes that occurred after the appearance of early angiosperms. Smaller genomes
316 and cells increased leaf surface conductance to CO_2 and enabled higher potential
317 and realized primary productivity. Interestingly, the physiological benefits of
318 small genomes and cells are realized only when photosynthetic rates are
319 proportional to transpiration rates; species employing CAM photosynthesis avoid
320 assimilating CO_2 during periods of high evaporative demand driven by light
321 interception. As a result, CAM species can have larger genomes without the
322 physiological costs that C3 species might incur. Additionally, CAM species often
323 inhabit marginal habitats characterized by limited water availability and nutrient
324 cycling that are unable to support high rates of primary productivity [49].
325 Furthermore, because genome downsizing lowers the limit of minimum cell size,
326 final cell size can vary much more widely, which facilitates a closer coupling of
327 anatomy and physiology with environmental conditions. Therefore, genome
328 downsizing has increased the range of habitable environments and allowed
329 angiosperms to outcompete other land plants in almost every ecosystem.
330

Methods

Leaf traits

Published data for guard cell length (l_g), stomatal density (D_s), and vein density (D_v) were compiled from the literature (Table S1). Genome size data for each species were taken from the Plant DNA C-values database (release 6.0, December 2012), managed by the Royal Botanic Gardens, Kew [22]. In total, our dataset comprised 1087 species of vascular plants, of which 979 were angiosperms, 54 were gymnosperms, and 54 were ferns. For the 979 angiosperms in the dataset, there were D_v data for 164 and guard cell size data for 220. Similarly, there were D_v data for 23 gymnosperms and for 10 ferns, and there were l_g data for 20 gymnosperms and for 41 ferns. The large discrepancy between the total number of angiosperms in the dataset and the number of angiosperms with leaf trait data is due to inclusion of genome size data for CAM species that lacked leaf trait data.

Because different photosynthetic pathways (C3, C4, CAM) employ different strategies of maintaining water balance, the effects of genome size-cell size allometry may differ among species employing different photosynthetic pathways. We tested this hypothesis by comparing genome size evolution among the angiosperms. We expected the largest difference to exist between C3 and CAM species, and so we focused the analysis on this comparison. The taxonomic distribution of CAM photosynthesis was based on Smith and Winter [23], which provides a list of genera exhibiting CAM photosynthesis. Undoubtedly, some of these genera include C3 species (either C3-CAM intermediates or exclusively C3), which would lead to a conservative estimate of the

differences in genome size between C3 and CAM species. Of the 973 angiosperms in this analysis, 271 were C3, nine were C4, and 647 were CAM.

Calculating maximum and operational stomatal conductance

For each species in our database with anatomical traits, we calculated the maximum stomatal conductance and the operational stomatal conductance. Maximum stomatal conductance ($g_{s,max}$) is defined by the dimensions of stomatal pores and their abundance, and represents the biophysical upper limit of gas diffusion through the leaf epidermis. Anatomical measurements of guard cells were used to calculate $g_{s,max}$ as [4,5]:

$$g_{s,max} = \frac{D_s \cdot a_{max} \frac{d_{H_2O}}{m_v}}{d_p + \frac{\pi}{2}\sqrt{a_{max}/\pi}} \quad (1)$$

where d_{H2O} is the diffusivity of water in air (0.0000249 m^2 s^{-1}), m_v is the molar volume of air normalized to 25 °C (0.0224 m^3 mol^{-1}), D_s is stomatal density (mm^{-2}), a_{max} is maximum stomatal pore size, and d_p is the depth of the stomatal pore. The a_{max} term can be approximated as: $\pi(l_p/2)^2$, where l_p is stomatal pore length with l_p being approximated as $l_g/2$, where l_g is guard cell length [4,24]. d_p is assumed to be equal to guard cell width (W). If W was not reported d_p was estimated as $0.36 \cdot l_g$ [7].

Operational stomatal conductance ($g_{s,op}$), by contrast, more accurately defines the stomatal conductance leaves attain under natural conditions when limitations in leaf hydraulic supply constrain stomatal conductance. We used an empirical model of $g_{s,op}$ [3] that directly relates D_v to stomatal conductance during periods of steady state transpiration as:

$$K_{leaf} = 12{,}670 d_m^{-1.27} \quad (2)$$

where:

$$d_m = {}^{\pi}/_{2}(d_x^2 + d_y^2)^{1/2} \quad (3)$$

$$d_x = 650/D_v \quad (4)$$

$$g_{s,\,op} = (K_{leaf}\,\Delta\Psi)/v \quad (5).$$

K_{leaf} is leaf hydraulic conductance (mmol m^{-2} s^{-1} MPa^{-1}), d_m is the post vein distance to stomata (μm), d_x is the maximum horizontal distance from vein to the stomata (μm), d_y is the distance from vein to the epidermis (μm), $\Delta\Psi$ is the water potential difference between stem and leaf (set to 0.33 MPa [25]) and v is vapor pressure deficit set to 2 kPa. In order to test the influence of variation in leaf thickness on $g_{s,\,op}$ we used three values of d_y (70, 100 and 130μm).

Analyses of trait evolution

To determine the temporal patterns of trait evolution, we generated a phylogeny from the list of taxa (Table S1) using Phylomatic (v. 3) and its stored family-level supertree (v. R20120829). To date nodes in the supertree, we compiled node ages from recent, fossil-calibrated estimates of crown group ages. Node ages were taken from Magallón et al. [26] for angiosperms, Lu et al. [27] for gymnosperms, and Testo and Sundue [28] for ferns. The age of all seed plants was taken as 330 million years [29]. Because there is

some uncertainty in the maximum age of the ancestor of all angiosperms, we took the angiosperm crown age used by Brodribb and Field [30] to make our results directly comparable to theirs. We tested this assumed angiosperm age by using different ages for the crown group angiosperms ranging from 130 Ma to 180 Ma, and the results were not qualitatively different. Of the 331 internal nodes in our tree, 90 of them had ages. These ages were assigned to nodes and all other branch lengths smoothed using the function 'bladj' in the software Phylocom (v. 4.2 [31]). Polytomies were resolved by random bifurcation and adding 5 million years to each of these new branches and subtracting an equivalent amount from the descending branches so that the tree remained ultrametric. For all subsequent analyses of character evolution, this method for randomly resolving polytomies was repeated 100 times to account for phylogenetic uncertainty. To fit models of trait evolution, stochastic character change [32] was mapped on each randomly resolved tree using the function 'make.simmap' in the R package *phytools* [33] before fitting each model of evolution (described below). For ancestral state reconstructions the ages and character estimates at each node were averaged across the 100 randomly resolved trees.

Ancestral state reconstructions were calculated using the residual maximum likelihood method, implemented in the function 'ace' from the R package *ape* [34]. To determine when changes in traits pushed the frontiers of trait values, the upper (D_v) and lower (genome size and l_g) limits of traits were estimated by first extracting the upper or lower ten percent of reconstructed trait values in sequential five million year windows and then attempting to fit curves to these values. This method is similar to a previous analysis of D_v evolution through time [35], which is included here for comparison. We compared three types of curve fits: a linear fit that lacked slope (equivalent to the mean of

the reconstructed trait values), a linear fit that included both a slope and an intercept, and a nonlinear curve of the form $trait = a + b/(1 + e^{(-(time + c)/d)})$. Curves were fit to reconstructed trait values for each clade between 160 and 50 Ma, which corresponds to the time period encompassing the major diversification and expansion of the angiosperms, and the best fit was chosen based on AIC scores with a difference in AIC of 5 taken to indicate significant differences in fits. Ancestral state reconstructions of genome size for CAM angiosperms were calculated separately from C3 and C4 angiosperms because of the computational time required for the analyses. Phylogenetic independent contrasts (PICs) were used to determine whether traits underwent correlated evolution. PICs for each pairwise combination of traits were calculated for only species with data for both traits. Correlations between PICs were calculated using Spearman rank correlations in the function 'cor.table' from the R package *picante* [36].

To determine whether the tempo and mode of genome size evolution differed among major clades and lineages with different photosynthetic pathways, we used the R package *mvMORPH* [37] to fit four types of evolutionary models under a maximum likelihood criterion: Brownian motion (BM) with a single rate of evolution for the entire tree, Brownian motion with multiple rates for different groups of taxa, Ornstein-Uhlenbeck (OU) process with a single adaptive optimum for all species, Ornstein-Uhlenbeck process with different trait optima for different groups of taxa. Three types of regimes were modeled: (1) C3 species in all three major clades, (2) angiosperms differing in photosynthetic pathway, (3) all clades and all photosynthetic pathways. In all of these analyses, we accounted for phylogenetic uncertainty as described above. Model fits were compared using AIC scores with a difference in AIC of 5 assumed to indicate a

446 significantly better model. In determining whether genome size evolution differed among
447 angiosperms with different photosynthetic pathways, we attempted to account for the
448 large discrepancy in the number of C3 and CAM angiosperms in the dataset by using all
449 species ('unbalanced' analysis) and by randomly sampling 271 CAM species so that there
450 were equivalent numbers of C3 and CAM species ('balanced' analysis). Then the same
451 models as above were fit and compared. Because the analysis focused on the comparison
452 between C3 and CAM species, *t*-tests were used to compare phylogenetic means and
453 rates of genome size evolution, although estimated parameters for C4 species are
454 included for completeness.

455 To determine whether there were temporal lags between changes in genome size
456 and changes in D_v and l_g, we compared OU models that allowed for multiple trait optima
457 that used symmetric (no time lag) and non-symmetric (one trait lags behind another)
458 alpha matrices. Although in univariate analyses the OU model underperformed the BM
459 models, analyses of time lags between trait shifts can be assessed using only OU models.
460
461 *Scaling relationships*
462 Scaling relationships between genome size and D_v, l_g, $g_{s,max}$, and $g_{s,op}$ were
463 calculated from log-transformed data and analyzed using the function 'sma' in the R
464 package *smatr* [36]. Analyses were performed for the entire dataset and also for individual
465 clades. Slope tests were used to determine whether the scaling relationship between
466 genome size and $g_{s,max}$ was significantly different than the relationship between genome
467 size and $g_{s,op}$ and whether the scaling relationship between genome size and $g_{s,op}$ and $g_{s,max}$
468 differed among clades.

469 Figure 1. The distribution of genome size among 1035 land plants. The family level
470 phylogeny has branches colored according to one random stochastic character map of
471 photosynthetic pathways (C3, C4, CAM) among clades (ferns, gymnosperms,
472 angiosperms). Orange bars at the tips are scaled proportional to genome size for each
473 terminal species.
474
475 Figure 2. Relationships between genome size and anatomical traits: (a) l_g, (b) D_s, and (c)
476 D_v. In all panels, insets show log-log relationships and R^2 values are from standard major
477 axis regressions. Correlations for phylogenetically corrected relationships are in Table
478 S2.
479
480 Figure 3. The relationships between genome size and maximum (solid line; $R^2 = 0.25$)
481 and operational (dashed lines) stomatal conductance, plotted on a log-log scale.
482 Operational stomatal conductance was modeled under assumptions of three leaf
483 thicknesses (70 μm, $R^2 = 0.46$; 100 μm, $R^2 = 0.44$; 130 μm, $R^2 = 0.43$). Points are
484 omitted for clarity. Correlations for phylogenetically corrected relationships are in Table
485 S2.
486
487 Figure 4. Ancestral state reconstructions of genome size, vein density (D_v), and guard
488 cell length (l_g) through time for angiosperms (colored circles), gymnosperms (grey
489 triangles), and ferns (grey squares). Error bars around reconstructed values represent
490 error due to phylogenetic uncertainty. The shaded timespan indicates the Cretaceous,
491 during which most major lineages of angiosperms diversified. Lines represent the best-fit

492 models through the lower (genome size and l_g) and upper (D_v) 10% of reconstructed
493 values. (a) Genome size was unchanged during the Cretaceous for the ferns (genome size
494 = 9.91, df = 2, P < 0.001) and the gymnosperms (genome size = 19.62, df = 2, P < 0.001),
495 while minimum genome size among the angiosperms decreased rapidly during the
496 Cretaceous (genome size = 0.99 + 3.06/(1 + e^(-time – 120.74)/9.03; df = 5, P < 0.001).
497 (b) Similar to the results of Brodribb and Field (2010), the upper limit of reconstructed D_v
498 through time increased significantly for the angiosperms (D_v = 3.93 + 5.29/(1 + e^(-(time
499 -124.47)/(-13.49)); df = 5, P < 0.001). However, vein densities of fern (D_v = 1.70; df = 2,
500 P < 0.01) and gymnosperm lineages (D_v = 1.68; df = 2, P < 0.001) remained unchanged
501 during the same time period. (c) Similarly, l_g declined rapidly among angiosperms (l_g =
502 23.64 + 13.82/(1 + e^(-(time -118.48)/9.31); df = 5, P < 0.001), while l_g of ferns (l_g =
503 42.52, df = 2, P < 0.001) and gymnosperms (l_g = 55.66, df = 2, P < 0.001) remained
504 unchanged during the Cretaceous. Marginal plots on the right represent the median
505 (points), interquartile ranges (solid lines) and ranges (dotted lines) of extant trait values.
506 Angiosperm data have been plotted separately for species exhibiting each photosynthetic
507 pathway. The two CAM gymnosperms were included with C3 gymnosperms in these
508 analyses.
509
510 Figure 5. Differences in reconstructed genome size and the rate of genome size evolution
511 for angiosperms differing in photosynthetic pathway. The reconstructed genome size and
512 the rate of genome size evolution differed among C3 and CAM species, regardless of
513 whether equivalent numbers of C3 and CAM species ('balanced', 271 species each) were
514 randomly sampled or whether all CAM species were included in the analysis

515 ('unbalanced'). The rate of genome size evolution is the Brownian motion rate parameter

516 calculated separately for each photosynthetic pathway. Points are medians, solid lines are

517 interquartile ranges, and dotted lines are ranges of modeled parameters.

518
519

Figure 1.

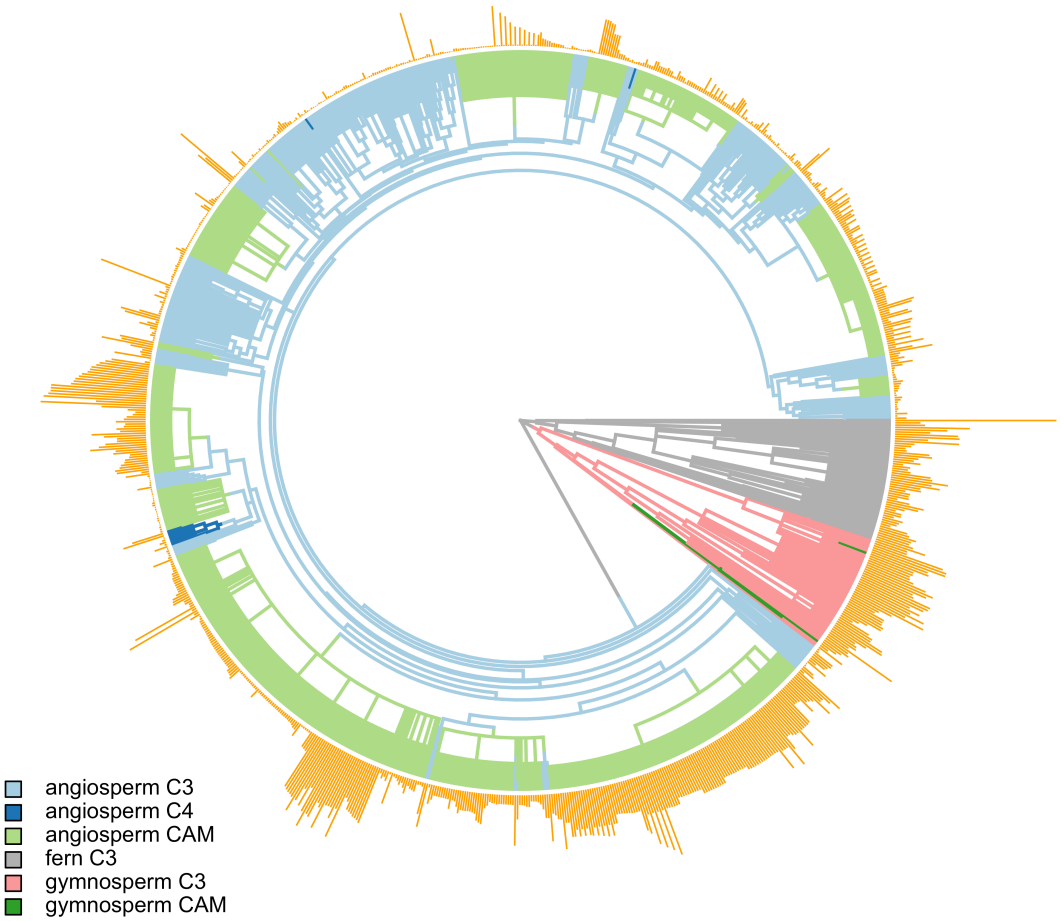

Figure 2.

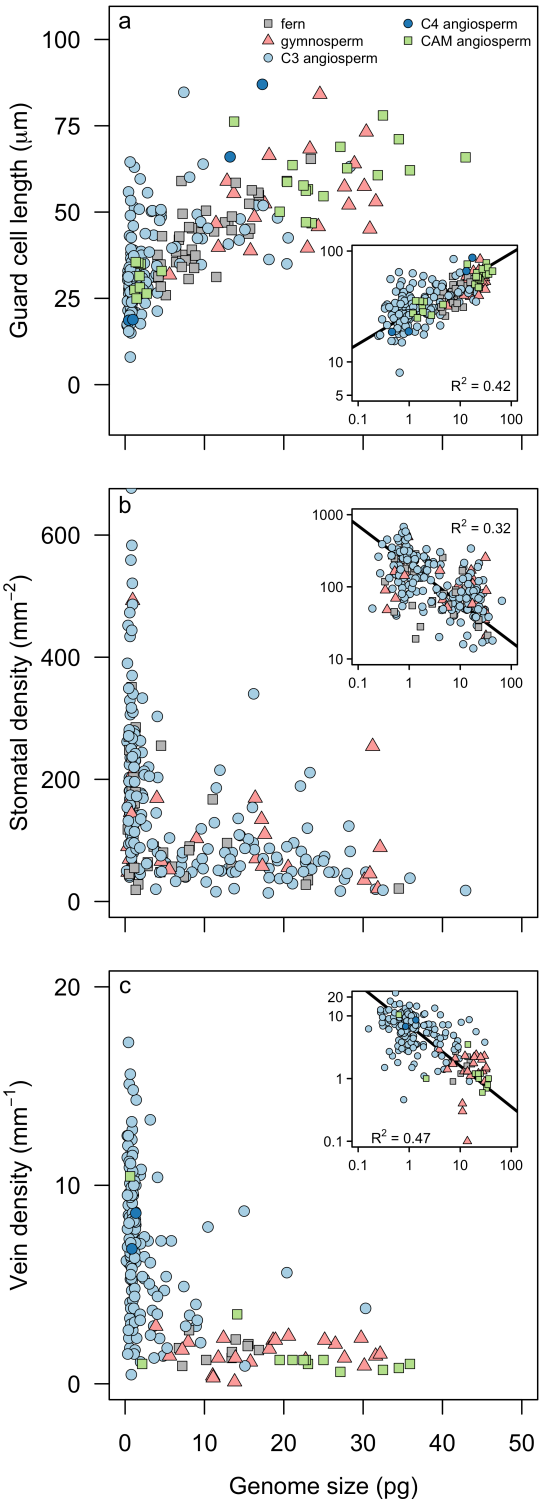

Figure 3.

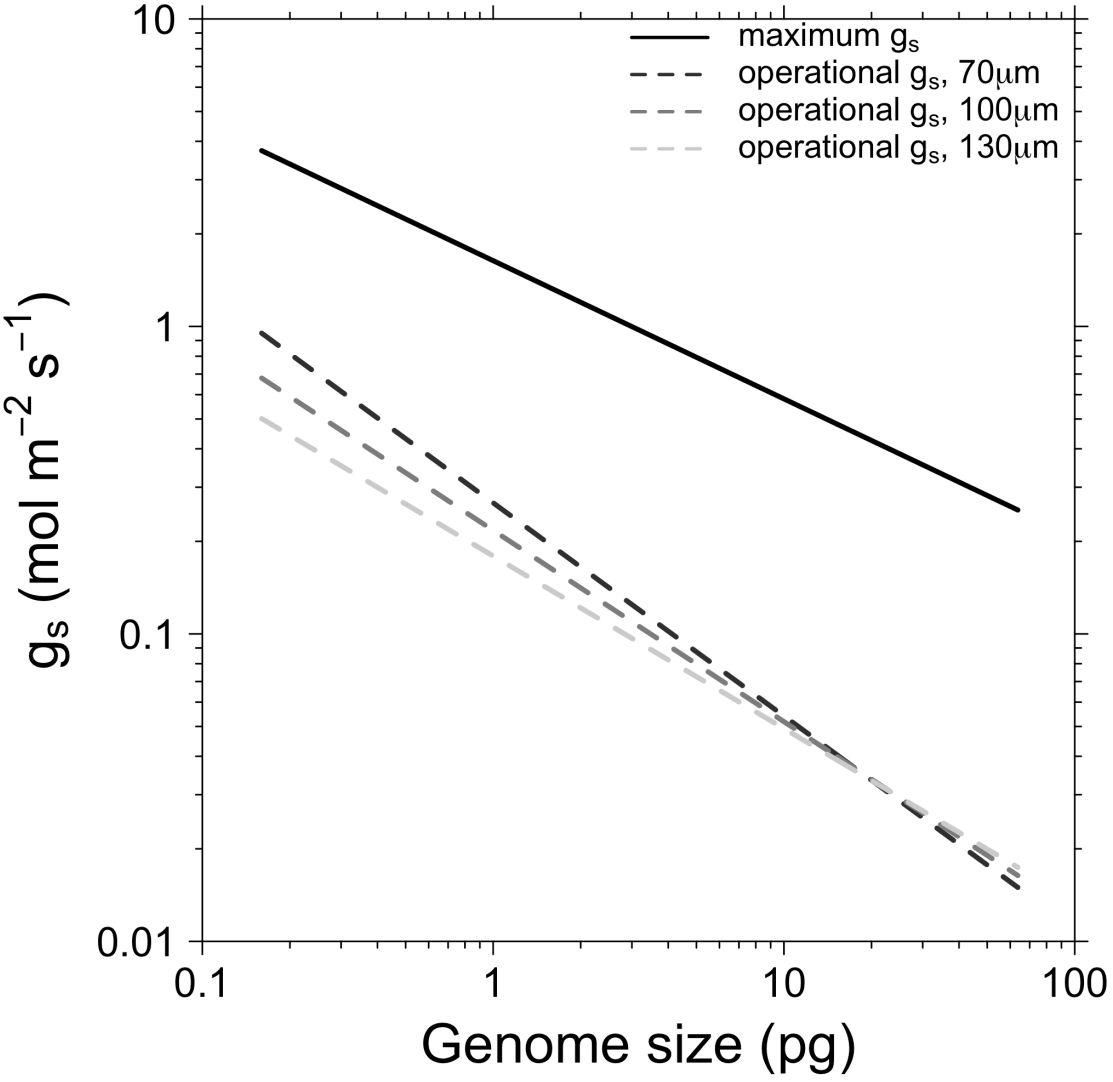

Figure 4.

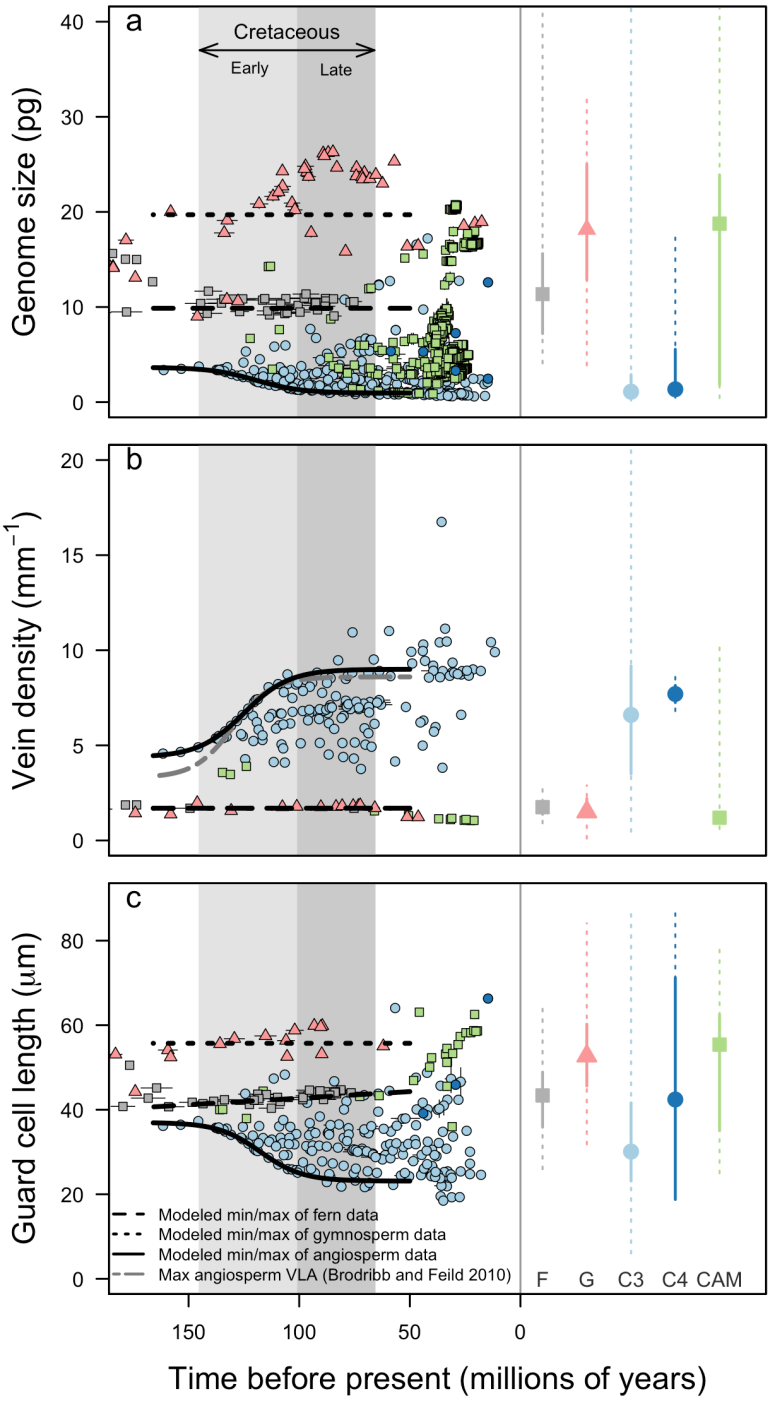

Figure 5.

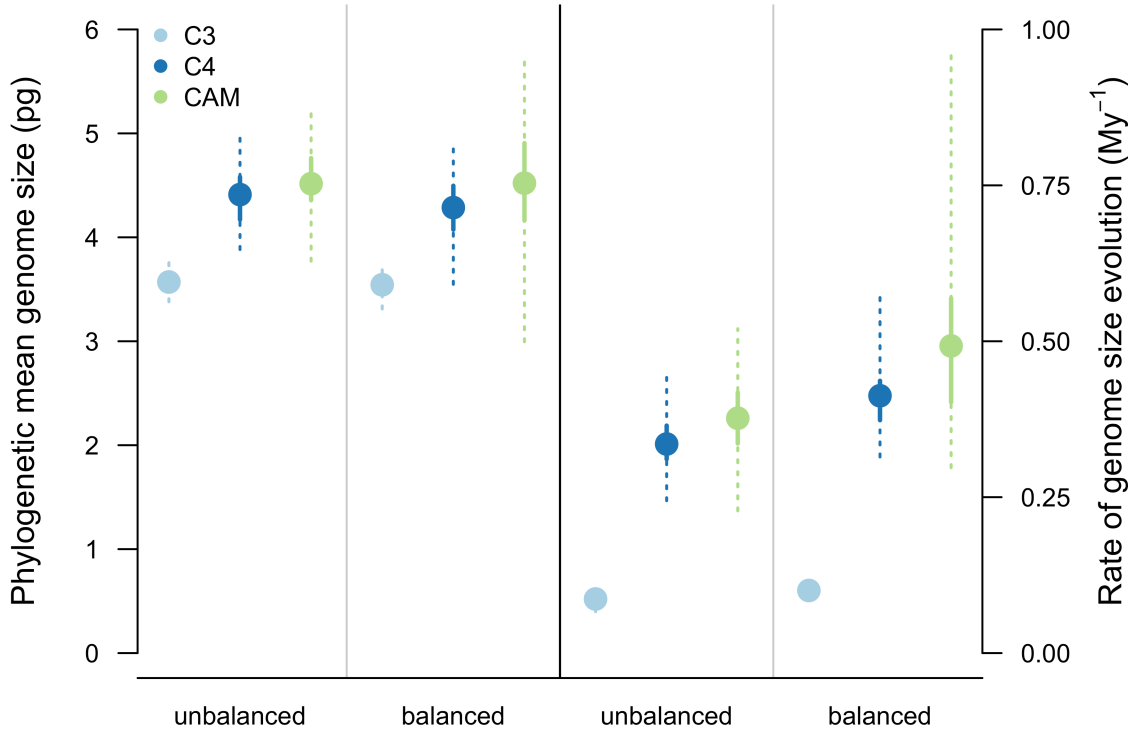

Table 1. Standard major axis regressions of D_v, l_g, $g_{s,max}$, and $g_{s,op}$ versus genome size for all species and for each clade separately. Asterisks indicate significance level: *P < 0.05; **P < 0.01; ***P < 0.001

	all			**angiosperm**			**gymnosperm**			**fern**		
	slope	intercept	R^2	slope	intercept	R^2	slope	intercept	R^2	slope	intercept	R^2
D_v	-0.646 (-0.716, -0.583)	0.848 (0.799, 0.897)	0.463 ***	-0.641 (-0.727, -0.566)	0.838 (0.789, 0.887)	0.329 ***	1.34 (0.864, 2.078)	-1.488 (-2.244, -0.732)	0.002	0.940 (0.454, 1.944)	-0.778 (-1.580, 0.025)	0.054
l_g	0.274 (0.249, 0.301)	1.435 (1.414, 1.456)	0.420 ***	0.300 (0.270, 0.333)	1.433 (1.411, 1.454)	0.477 ***	0.529 (0.354,0.792)	1.036 (0.749, 1.324)	0.300 *	0.480 (0.383, 0.602)	1.167 (1.060, 1.274)	0.523 ***
$g_{s,max}$	-0.449 (-0.509, -0.397)	0.214 (0.167, 0.260)	0.245 ***	-0.447 (-0.514, -0.388)	0.208 (0.160, 0.255)	0.170 ***	1.178 (0.668, 2.078)	-1.750 (-2.646, -0.854)	0.004	0.971 (0.425, 2.221)	-1.201 (-2.11, -0.288)	0.352
$g_{s,op}$ 70µm	-0.693 (-0.769, -0.625)	-0.573 (-0.626, -0.522)	0.457 ***	-0.662 (-0.750, -0.584)	-0.586 (-0.635, -0.536)	0.335 ***	1.605 (1.010, 2.551)	-3.295 (-4.252, -2.338)	0.001	1.169 (0.566, 2.415)	-2.473 (-3.468, -1.479)	0.060

Table 2. Univariate evolutionary modeling of genome size was best fit by a Brownian motion model with multiple rates. Parameter values are means ± standard error of 100 replicate simulations accounting for phylogenetic uncertainty. θ = genome size at the phylogenetic root, σ^2= rate of evolution.

Angiosperms: genome size							
	θ	σ^2		Log-likelihood	AIC	Delta(AIC)	
C3	3.57 ± 0.008	0.087 ± 0.0006		-2749.6 ± 1.73	5511.2 ± 3.47	102.39 ± 1.04	
C4	4.39 ± 0.03	0.339 ± 0.0004					
CAM	4.52 ± 0.03	0.380 ± 0.006					
All clades: genome size							
Ferns	20.33 ± 0.009	0.194 ± 0.0009		-1074.2 ± 0.32	2160.4 ± 0.64	14.34 ± 0.17	
Gymnosperms	15.17 ± 0.008	0.140 ± 0.0008					
Angiosperms	3.53 ± 0.005	0.088 ± 0.0006					
All clades and pathways: Genome size							
Ferns	20.35 ± 0.008	0.194 ± 0.001		-3102.92 ± 1.771	6229.84 ± 3.542	130.14 ± 1.20	
C3 Gymnosperms	15.00 ± 0.008	0.136 ± 0.001					
CAM Gymnosperms	15.12 ± 0.030	0.0005 ± 0.0005					
C3	3.58 ±	0.087 ±					

angiosperms	0.009	0.001					
C4 angiosperms	4.33 ± 0.031	0.341 ± 0.004					
CAM angiosperms	4.52 ± 0.031	0.380 ± 0.006					

Table S2. Trait and phylogenetic independent contrast (PIC) correlations for all species and for only the angiosperms. Trait correlations are in the upper triangle and contrast correlations in the lower triangle. Spearman rank correlation coefficients are shown. Asterisks indicate significance level: *P < 0.05; **P < 0.01; ***P < 0.001

All species					
	Genome size	D_v	l_g	$g_{s,\ max}$	$g_{s,\ op\ 70}$
Genome size		-0.65***	0.74***	-0.46***	-0.65***
D_v	-0.16*		-0.63***	0.67***	0.99***
l_g	0.46***	-0.25*		-0.31***	-0.63***
$g_{s,\ max}$	-0.15*	0.35**	0.01		0.67***
$g_{s,\ op\ 70}$	-0.19**	0.99***	-0.25*	0.37**	
Angiosperms					
Genome size		-0.48***	0.65***	-0.34***	-0.49***
D_v	-0.16*		-0.56***	0.59***	0.99***
l_g	0.45***	-0.22		-0.23***	-0.56***
$g_{s,\ max}$	-0.17*	0.32*	0.04		0.59***
$g_{s,\ op\ 70}$	-0.19*	0.99***	-0.22	0.35**	

Table S1 References

1. Ahmad, K., Khan, M. A., Ahmad, M. & Zafar, M. Taxonomic diversity of stomata in dicot flora of a district tank (N.W.F.P.) in Pakistan. *African journal of ...* **8,** 1052–1055 (2009).
2. Álvarez, S. G., Amorena, I. G., Rubiales, J. M. & Morla, C. The value of leaf cuticle characteristics in the identification and classification of Iberian Mediterranean members of the genus Pinus. *Botanical Journal of the Linnean Society* **161,** 436–448 (2009).
3. Barrington, D. S., Paris, C. A. & Ranker, T. A. Systematic inferences from spore and stomate size in the ferns. *American Fern Journal* **76,** 149–159 (1986).
4. Beaulieu, J. M., Leitch, I. J., Patel, S., Pendharkar, A. & Knight, C. A. Genome size is a strong predictor of cell size and stomatal density in angiosperms. *New Phytologist* **179,** 975–986 (2008).
5. Blonder, B. & Enquist, B. J. Inferring climate from angiosperm leaf venation networks. *New Phytologist* **204,** 116–126 (2014).
6. Blonder, B., Violle, C., Bentley, L. P. & Enquist, B. J. Venation networks and the origin of the leaf economics spectrum. *Ecol Lett* **14,** 91–100 (2010).
7. Boyce, C. K., Brodribb, T. J., Feild, T. S. & Zwieniecki, M. A. Angiosperm leaf vein evolution was physiologically and environmentally transformative. *P R Soc B* **276,** 1771–1776 (2009).
8. Walls, R. Angiosperm leaf vein patterns are linked to leaf functions in a global-scale data set. *American Journal of Botany* **98,** 244–253 (2011).
9. Zonneveld, B. J. M. & Lindström, A. J. Genome sizes for 71 species of Zamia(Cycadales: Zamiaceae) correspond with three different biogeographic regions. *Nordic Journal of Botany* **34,** 744–751 (2016).
10. Carpenter, S. B. & Smith, N. D. Stomatal distribution and size in southern Appalachian hardwoods. *Can J Bot* **53,** 1153–1156 (1975).
11. Brodribb, T. J. & Feild, T. S. Leaf hydraulic evolution led a surge in leaf photosynthetic capacity during early angiosperm diversification. *Ecol Lett* **13,** 175–183 (2010).
12. Carpenter, K. J. Stomatal architecture and evolution in basal angiosperms. *American Journal of Botany* **92,** 1595–1615 (2005).
13. Jordan, G. J., Carpenter, R. J., Koutoulis, A., Price, A. & Brodribb, T. J. Environmental adaptation in stomatal size independent of the effects of genome size. *New Phytologist* **205,** 608–617 (2015).
14. Scoffoni, C., Rawls, M., McKown, A., COCHARD, H. & Sack, L. Decline of Leaf Hydraulic Conductance with Dehydration: Relationship to Leaf Size and Venation Architecture. *Plant Physiology* **156,** 832–843 (2011).
15. Coomes, D. A., Heathcote, S., Godfrey, E. R., Shepherd, J. J. & Sack, L. Scaling of xylem vessels and veins within the leaves of oak species. *Biology Letters* **4,** 302–306 (2008).
16. de Boer, H. J. *et al.* Optimal allocation of leaf epidermal area for gas exchange. *New Phytologist* **210,** 1219–1228 (2016).
17. Delucia, E. H. & Berlyn, G. P. The effect of increasing elevation on leaf cuticle thickness and cuticular transpiration in balsam fir. *Can J Bot* **62,** 2423–2431 (1984).
18. Franks, P. J. & Beerling, D. J. CO2-forced evolution of plant gas exchange capacity and water-use efficiency over the Phanerozoic. *Geobiology* **7,** 227–236 (2009).

19. Gleason, S. M. *et al.* Weak coordination among petiole, leaf, vein, and gas-exchange traits across Australian angiosperm species and its possible implications. *Ecology and Evolution* **6,** 267–278 (2016).
20. Gola, E. M. & Szczesniak, E. in *Genus Polypodium L.* (eds. Szczesniak, E. & Gola, E. M.) 39–46 (Polish Botanical Society, 2012).
21. Haworth, M., Heath, J. & McElwain, J. C. Differences in the response sensitivity of stomatal index to atmospheric CO2 among four genera of Cupressaceae conifers. *Ann Bot-London* **105,** 411–418 (2010).
22. Haworth, M., Fitzgerald, A. & Mcelwain, J. C. Cycads show no stomatal-density and index response to elevated carbon dioxide and subambient oxygen. *Aust J Bot* **59,** 630 (2011).
23. Haworth, M., Killi, D., Materassi, A. & Raschi, A. Coordination of stomatal physiological behavior and morphology with carbon dioxide determines stomatal control. *American Journal of Botany* **102,** 677–688 (2015).
24. Henry, T. A., Bainard, J. D., Newmaster, S. G. & Schwarzacher, T. Genome size evolution in Ontario ferns (Polypodiidae): evolutionary correlations with cell size, spore size, and habitat type and an absence of genome downsizing. *Genome* **57,** 555–566 (2014).
25. McElwain, J. C., Yiotis, C. & Lawson, T. Using modern plant trait relationships between observed and theoretical maximum stomatal conductance and vein density to examine patterns of plant macroevolution. *New Phytologist* **209,** 94–103 (2015).
26. Mehra, P. N. & Soni, S. L. Stomatal patterns in pteridophytes - an evolutionary approach. *Proceedings of the Indian National Science Academy* **B49,** 155–203 (1983).
27. Nardini, A., Gortan, E. & Salleo, S. Hydraulic efficiency of the leaf venation system in sun- and shade-adapted species. *Functional Plant Biol.* **32,** 953–961 (2005).
28. Nardini, A., Pedà, G. & Rocca, N. L. Trade-offs between leaf hydraulic capacity and drought vulnerability: morpho-anatomical bases, carbon costs and ecological consequences. *New Phytologist* **196,** 788–798 (2012).
29. Ogaya, R., Llorens, L. & Peñuelas, J. Density and length of stomatal and epidermal cells in "living fossil" trees grown under elevated CO_2 and a polar light regime. *Acta Oecologica* **37,** 381–385 (2011).
30. Pérez-Farrera, M. A., Vovides, A. P. & Avendaño, S. Morphology and Leaflet Anatomy of the Ceratozamia norstogii(Zamiaceae, Cycadales) Species Complex in Mexico with Comments on Relationships and Speciation. *Int J Plant Sci* **175,** 110–121 (2014).
31. Reed, J. E. & Smith, W. K. Stomatal Frequency, Distribution, and Needle Hydrophobicity in Cloud Forest Spruce and Fir, Southern Appalachian Mountains. *RURALS: Review of Undergraduate Research in Agricultural and Life Sciences* **7,** 1–12 (2012).
32. Sack, L. & Frole, K. Leaf structural diversity is related to hydraulic capacity in tropical rain forest trees. *Ecology* **87,** 483–491 (2006).
33. Tiwari, S. P., Kumar, P. & Yadav, D. Comparative morphological, epidermal, and anatomical studies of *Pinus roxburghii* needles at different altitudes in the North-West Indian Himalayas. *Turkish Journal of …* **37,** 65–73 (2013).
34. Vovides, A. P., Etherington, J. R. & Dresser, P. Q. CAM-cycling in the cycad Dioon edule Lindl. in its natural tropical deciduous forest habitat in central Veracruz, Mexico. *Botanical Journal of …* **138,** 155–162 (2002).

35. Wang, R. *et al.* Elevation-Related Variation in Leaf Stomatal Traits as a Function of Plant Functional Type: Evidence from Changbai Mountain, China. *PLoS ONE* **9,** e115395 (2014).
36. Zhang, S.-B. *et al.* Evolutionary Association of stomatal traits with leaf vein density in *Paphiopedilum*, Orchidaceae. *PLoS ONE* **7,** e40080 (2012).
37. Zwieniecki, M. A. & Boyce, C. K. Evolution of a unique anatomical precision in angiosperm leaf venation lifts constraints on vascular plant ecology. *P R Soc B* **281,** 20132829–20132829 (2014).
38. Colmer, T. D. & Pedersen O. Underwater photosynthesis and respiration in leaves of submerged wetland plants: gas films improve CO2 and O2 exchange. *New Phytologist* **177,** 918 - 926 (2008).
39. Plymale, E. L. & Wylie, R. B. The major veins of mesomorphic leaves. *American Journal of Botany* **31,** 99 - 106 (1944).
40. Sack, L., Scoffoni, C., McKown, A. D., Frole, K., Rawls, M., Havran J. C., Tran, H. & Tran, T. Developmentally based scaling of leaf venation architecture explains global ecological patterns. *Nature Communications* **3**, 837 (2012).
41. Feild, T. S., Upchurch, G. R., Chatelet, D. S., Brodribb, T. J., Grubbs, K. C., Samain, M-S. & Wanke S. Fossil evidence for low gas exchange capacities for early cretaceous angiosperm leaves. *Paleobiology* **37,** 195 - 213 (2016).
42. Weryszko-Chielewska, E. & Haratym, W. Leaf micromorphology of *Aesculus hippocastanum* L. and damage caused by leaf-mining larvae of *Cameraria ohridella* Deschka & Dimic. *Acta Agrobotanica* **65,** 25 - 34 (2012).
43. Brodribb, T. J., Jordan G. J. & Carpenter, R. J. Unified changes in cell size permit coordinated leaf evolution. *New Phytologist* **199,** 559 - 570 (2013).
44. Ekrt, L., Trávníček, P., Jarmolímová, V., Vít, P. & Urfus, T. Genome size and morphology of the *Drypoteris affinis* group in Central Europe. *Preslia* **81,** 261 - 280 (2009).
45. Jordan, G. J., Brodribb, T. J., Blackman, C. J. & Weston, P. H. Climate drives vein anatomy in Proteaceae. *American Journal of Botany* **100,** 1483 - 1493 (2013).
46. Walls, R. L. Angiosperm leaf vein patterns are linked to leaf functions in a global-scale data set. *American Journal of Botany* **98,** 244 - 253 (2011).
47. Darbyshire, S. J. & Francis, A. The biology of invasive alien plants in Canada. 10. *Nymphoides peltata* (S. G. Gmel.) Kuntze. *Canadian Journal of Plant Science* **88,** 811 - 829 (2008).
48. Fiorin, L. Spatial coordination between veins and stomata links water supply with water loss in leaves. PhD dissertation, University of Padova, January (2013).

Article References

1. Friedman, W. E. The meaning of Darwin's "abominable mystery". *American Journal of Botany* **96,** 5–21 (2009).
2. Augusto, L., Davies, T. J., Delzon, S. & De Schrijver, A. The enigma of the rise of angiosperms: can we untie the knot? *Ecol Lett* **17,** 1326–1338 (2014).
3. Brodribb, T. J., Feild, T. S. & Jordan, G. J. Leaf Maximum Photosynthetic Rate and Venation Are Linked by Hydraulics. *Plant Physiology* **144,** 1890–1898 (2007).
4. Franks, P. J. & Beerling, D. J. Maximum leaf conductance driven by CO2 effects on stomatal size and density over geologic time. *Proceedings of the National Academy of Sciences* **106,** 10343–10347 (2009).
5. Franks, P. J. & Farquhar, G. D. The effect of exogenous abscisic acid on stomatal development, stomatal mechanics, and leaf gas exchange in Tradescantia virginiana. *Plant Physiology* **125,** 935–942 (2001).
6. Sack, L. & Buckley, T. N. The developmental basis of stomatal density and flux. *Plant Physiology* **171,** 2358–2363 (2016).
7. de Boer, H. J. *et al*. Optimal allocation of leaf epidermal area for gas exchange. *New Phytologist* **210,** 1219–1228 (2016).
8. John, G. P., Scoffoni, C. & Sack, L. Allometry of cells and tissues within leaves. *American Journal of Botany* **100,** 1936–1948 (2013).
9. de Boer, H. J., Eppinga, M. B., Wassen, M. J. & Dekker, S. C. A critical transition in leaf evolution facilitated the Cretaceous angiosperm revolution. *Nature Communications* **3,** 1–11 (2012).
10. Carins Murphy, M. R., Jordan, G. J. & Brodribb, T. J. Differential leaf expansion can enable hydraulic acclimation to sun and shade. *Plant Cell Environ* **35,** 1407–1418 (2012).
11. Feild, T. S. & Brodribb, T. J. Hydraulic tuning of vein cell microstructure in the evolution of angiosperm venation networks. *New Phytologist* **199,** 720–726 (2013).
12. Mirsky, A. E. & Ris, H. The desoxyribonucleic acid content of animal cells and its evolutionary significance. *J. Gen. Physiol.* **34,** 451–462 (1951).
13. Cavalier-Smith, T. Nuclear volume control by nucleoskeletal DNA, selection for cell volume and cell growth rate, and the solution of the DNA C-value paradox. *J Cell Sci* **34,** 247–278 (1978).
14. Simova, I. & Herben, T. Geometrical constraints in the scaling relationships between genome size, cell size and cell cycle length in herbaceous plants. *P R Soc B* **279,** 867–875 (2012).
15. Beaulieu, J. M., Leitch, I. J., Patel, S., Pendharkar, A. & Knight, C. A. Genome size is a strong predictor of cell size and stomatal density in angiosperms. *New Phytologist* **179,** 975–986 (2008).
16. Leitch, I. J. Evolution of DNA Amounts Across Land Plants (Embryophyta). *Ann Bot-London* **95,** 207–217 (2005).
17. Jiao, Y. *et al*. Ancestral polyploidy in seed plants and angiosperms. *Nature* **473,** 97–100 (2011).
18. Bennett, M. D. Nuclear DNA content and minimum generation time in herbaceous plants. *Proc. R. Soc. Lond., B, Biol. Sci.* **181,** 109–135 (1972).
19. Bennett, M. D. Variation in genomic form in plants and its ecological implications. *New Phytologist* **106,** 177–200 (1987).
20. Hodgson, J. G. *et al*. Stomatal vs. genome size in angiosperms: the somatic tail wagging

the genomic dog? *Ann Bot-London* **105,** 573–584 (2010).
21. Franks, P. J., Freckleton, R. P., Beaulieu, J. M., Leitch, I. J. & Beerling, D. J. Megacycles of atmospheric carbon dioxide concentration correlate with fossil plant genome size. *Philos T R Soc B* **367,** 556–564 (2012).
22. *Plant DNA C-values database*. (kew, 2012). Available at: http://data.kew.org/cvalues/. (Accessed: 15 February 2017)
23. Smith, J. & Winter, K. in *Crassulacean Acid Metabolism Biochemistry, Ecophysiology and Evolution* (eds. Winter, K. & Smith, A. J.) 427–436 (Crassulacean acid metabolism, 1996).
24. Franks, P. J. & Farquhar, G. D. The mechanical diversity of stomata and its significance in gas-exchange control. *Plant Physiology* **143,** 78–87 (2007).
25. Simonin, K. A., Limm, E. B. & Dawson, T. E. Hydraulic conductance of leaves correlates with leaf lifespan: implications for lifetime carbon gain. *New Phytologist* **193,** 939–947 (2012).
26. Magallón, S., Gómez-Acevedo, S., Sánchez-Reyes, L. L. & Hernández-Hernández, T. A metacalibrated time-tree documents the early rise of flowering plant phylogenetic diversity. *New Phytologist* **207,** 437–453 (2015).
27. Lu, Y., Ran, J.-H., Guo, D.-M., Yang, Z.-Y. & Wang, X.-Q. Phylogeny and Divergence Times of Gymnosperms Inferred from Single-Copy Nuclear Genes. *PLoS ONE* **9,** e107679 (2014).
28. Testo, W. & Sundue, M. Molecular Phylogenetics and Evolution. *Molecular Phylogenetics and Evolution* **105,** 200–211 (2016).
29. Magallon, S., Hilu, K. W. & Quandt, D. Land plant evolutionary timeline: Gene effects are secondary to fossil constraints in relaxed clock estimation of age and substitution rates. *American Journal of Botany* **100,** 556–573 (2013).
30. Brodribb, T. J. & Feild, T. S. Leaf hydraulic evolution led a surge in leaf photosynthetic capacity during early angiosperm diversification. *Ecol Lett* **13,** 175–183 (2010).
31. Webb, C. O., Ackerly, D. D. & Kembel, S. W. Phylocom: software for the analysis of phylogenetic community structure and trait evolution. *Bioinformatics* **24,** 2098–2100 (2008).
32. Huelsenbeck, J. P., Nielsen, R. & Bollback, J. P. Stochastic Mapping of Morphological Characters. *Systematic Biology* **52,** 131–158 (2003).
33. Revell, L. J. phytools: an R package for phylogenetic comparative biology (and other things). *Methods Ecol Evol* **3,** 217–223 (2011).
34. Paradis, E., Claude, J. & Strimmer, K. APE: Analyses of Phylogenetics and Evolution in R language. *Bioinformatics* **20,** 289–290 (2004).
35. Feild, T., Brodribb, T. & Iglesias, A. Fossil evidence for Cretaceous escalation in angiosperm leaf vein evolution. *Proceedings of the National Academy of Sciences* **108,** 8363–8366 (2011).
36. Kembel, S. W. *et al*. Picante: R tools for integrating phylogenies and ecology. *Bioinformatics* **26,** 1463–1464 (2010).
37. Clavel, J., Escarguel, G. & Merceron, G. mv morph: an rpackage for fitting multivariate evolutionary models to morphometric data. *Methods Ecol Evol* **6,** 1311–1319 (2015).
38. Franks, P. J., Leitch, I. J., Ruszala, E. M., Hetherington, A. M. & Beerling, D. J. Physiological framework for adaptation of stomata to CO2 from glacial to future concentrations. *Philos T R Soc B* **367,** 537–546 (2012).

39. Coomes, D. A., Heathcote, S., Godfrey, E. R., Shepherd, J. J. & Sack, L. Scaling of xylem vessels and veins within the leaves of oak species. *Biology Letters* **4,** 302–306 (2008).
40. Pittermann, J., Sperry, J., Hacke, U., Wheeler, J. & Sikkema, E. Torus-Margo Pits Help Conifers Compete with Angiosperms. *Science* **310,** 1924–1924 (2005).
41. Boyce, C. K. & Lee, J.-E. Could Land Plant Evolution Have Fed the Marine Revolution? *Paleontological Research* **15,** 100–105 (2011).
42. Boyce, C. K., Brodribb, T. J., Feild, T. S. & Zwieniecki, M. A. Angiosperm leaf vein evolution was physiologically and environmentally transformative. *P R Soc B* **276,** 1771–1776 (2009).
43. Sanderson, M. J. & Donoghue, M. J. Shifts in diversification rate with the origin of angiosperms. *Science* **264,** 1590–1593 (1994).
44. Labandeira, C. C. & Currano, E. D. The Fossil Record of Plant-Insect Dynamics. *Annu Rev Earth Pl Sc* **41,** 287–311 (2013).
45. Crepet, W. L. & Niklas, K. J. Darwin's second "abominable mystery": Why are there so many angiosperm species? *American Journal of Botany* **96,** 366–381 (2009).
46. Fenster, C. B., Armbruster, W. S., Wilson, P., Dudash, M. R. & Thomson, J. D. Pollination Syndromes and Floral Specialization. *Annu Rev Ecol Evol S* **35,** 375–403 (2004).
47. Labandeira, C. C., Dilcher, D. L., Davis, D. R. & Wagner, D. L. Ninety-seven million years of angiosperm-insect association: paleobiological insights into the meaning of coevolution. *P Natl Acad Sci Usa* **91,** 12278–12282 (1994).
48. Berendse, F. & Scheffer, M. The angiosperm radiation revisited, an ecological explanation for Darwin's 'abominable mystery'. *Ecol Lett* **12,** 865–872 (2009).
49. Ehleringer, J. R. & Monson, R. K. Evolutionary and ecological aspects of photosynthetic pathway variation. *Annual Review of Ecology and Evolution* **24,** 411–439 (1993).